Published in final edited form as:

Anal Biochem. 2008 June 15; 377(2): 141–149. doi:10.1016/j.ab.2008.03.034.

Fluorescence Intensity Decays of 2-Aminopurine solutions: Lifetime Distribution Approach

Shashank Bharill[1], **Pabak Sarkar**[1], **Jeff D. Ballin**[2], **Ignacy Gryczynski**[1], **Gerald M. Wilson**[2], and **Zygmunt Gryczynski**[1]

[1]Center for Commercialization of Fluorescence Technologies, Department of Molecular Biology and Immunology, Department of Cell Biology and Genetics, University of North Texas Health Science Center, Fort Worth, Texas – 76107.

[2]Department of Biochemistry and Molecular Biology and Marlene and Stewart Greenebaum Cancer Center, University of Maryland School of Medicine, 108 N. Greene St., Baltimore, Maryland - 21201.

Abstract

The fluorescent adenine analogue 2-aminopurine (2AP) has been used extensively to monitor conformational changes and macromolecular binding events involving nucleic acids because its fluorescence properties are highly sensitive to changes in chemical environment. Furthermore, site-specific incorporation of 2AP permits local DNA and RNA conformational events to be discriminated from the global structural changes monitored by UV/Vis spectroscopy and circular dichroism. However, while the steady-state fluorescence properties of 2AP have been well defined in diverse settings, interpretation of 2AP fluorescence lifetime parameters has been hampered by the heterogeneous nature of multi-exponential 2AP intensity decays observed across populations of microenvironments. To resolve this problem, we have tested the utility of multi-exponential versus continuous Lorentzian lifetime distribution models to describe fluorescence intensity decays from 2AP in diverse chemical backgrounds and within the context of RNA. Heterogeneity was introduced into 2AP intensity decays by mixing solvents of differing polarities, or by adding quenchers under high viscosity to evaluate the transient effect. Heterogeneity of 2AP fluorescence within the context of a synthetic RNA hairpin was introduced by structural remodeling using a magnesium salt. In each case, except folded RNA which required a bimodal distribution, 2AP lifetime properties were well described by single Lorentzian distribution functions, abrogating the need to introduce additional discrete lifetime subpopulations. Rather, heterogeneity in fluorescence decay processes was accommodated by the breadth of each distribution. This approach also permitted solvent relaxation effects on 2AP emission to be assessed by comparing lifetime distributions at multiple wavelengths. Together, these studies provide a new perspective for the interpretation of 2AP fluorescence lifetime properties, which will further the utility of this

To whom correspondence should be addressed: Dr. Zygmunt Gryczynski, CCFT, Department of Molecular Biology and Immunology, University of North Texas Health Science Center, 3500 Camp Bowie Blvd, Fort Worth, Texas, 76107. Telephone: 817-735-5471. Fax: 817-735-2119. zgryczyn@hsc.unt.edu.

fluorophore in analyses of the complex and heterogeneous structural microenvironments associated with nucleic acids.

Keywords

2-Aminopurine; Nucleic acids; Lifetime distribution; Transient effect; Solvent relaxation

1. INTRODUCTION

Interactions between proteins and nucleic acids are often accompanied by changes in local nucleic acid structures. There is a growing interest in characterizing both the nature and dynamics of these changes, which have important implications for the consequences and regulation of these binding events. This is particularly relevant for RNA-protein interactions, since RNA molecules can exhibit a diverse array of structural features under physiological conditions [1,2]. Fluorescence-based approaches offer a powerful approach to monitor macromolecular conformational changes in solution; however, the intrinsic fluorescence of nucleic acid bases is too weak to assess nucleic acid conformational events directly. Furthermore, the absorption/excitation of the bases are in the UV region where the emission is usually dominated by tryptophan and tyrosine fluorescence from the proteins. Although exciting progress has been made in the development of fluorescent dyes for spectroscopy and microscopy, these extrinsic probes are quite large and can significantly disturb the structure and stability of folded nucleic acids, particularly when positioned internally. As a result of these limitations, 2-aminopurine (2AP), a strongly fluorescent analog of adenine, has been used frequently to study local conformational changes in nucleic acids [3–5].

There are several advantages for using 2AP as a DNA/RNA fluorescent probe. First, longer wavelength absorption allows excitation above 300 nm (outside Trp/Tyr absorption). Second, the structures of DNA and RNA are minimally affected by replacing adenine with 2AP [5,6]. Third, fluorescence emission from 2AP strongly depends on local environment [7, 8] and is quenched by neighboring bases in DNA/RNA. 2AP has been successfully used to study interaction of DNA and RNA with proteins [9– 13], repair enzymes [14–16], folding of ribozymes [17], DNA damage and mismatching [18,19].

For about three decades the spectroscopic properties of 2AP have been investigated by several laboratories. The ground and lowest electronic excited states have a π-π^* character [20]. In aqueous solutions the quantum efficiency is about 0.7 [3], maxima of absorption and emission are about 305 nm and 370 nm respectively [4,21] and the fluorescence intensity decays are mono-exponential with the fluorescence lifetime of about 12 ns [8,22]. pH has not been found to have any effect on absorption and emission of 2AP, indicating its single protonation state in neutral solution [3,22].

Despite the use of 2AP in many biophysical and biochemical studies, the effects of many molecular interactions inherent to nucleic acid chemistry on the spectroscopic properties of 2AP remain poorly defined. Some interactions, like aromatic stacking with guanine, quench the fluorescence of 2AP by electron transfer processes [23]. However, less is understood about the effects of many other common nucleic acid structural features on 2AP

fluorescence, including hydrogen bonding and perturbations of local solvent interactions. The latter parameter can be assessed using binary solvent mixtures (mixture of polar and non-polar solvent); this strategy has shown that the composition of the solvation shell significantly influences the spectral properties and decay of fluorophores [7]. Several groups have used fluorescence lifetime analyses and anisotropy decays to track changes in the local environment of 2AP [24,25]. However, the interpretation of these time-resolved measurements has proven difficult, since the variety of possible 2AP microenvironments within nucleic acid structures imparts often complex multi-exponential decay properties to 2AP lifetimes. These microenvironments can be due to the degree of stacking with neighboring bases, the identity of those interacting bases, as well as varying nucleic acid structural subpopulations and degrees of solvent exposure. Together, this broad array of possible microenvironments would be expected to introduce significant heterogeneity into 2AP lifetime properties, further complicating interpretation of these data.

In this report, we provide evidence that fluorescence lifetime distribution models provide a robust and useful alternative to multi-exponential analysis of 2AP lifetimes in heterogeneous chemical environments and in a relevant biological system. Lifetime distribution describes intensity decays where total decay is the sum of individual decays weighted by amplitude. Consequently, one can fit a complex decay with fewer exponential components. Here, we demonstrate the utility of lifetime distributions when various conformations of fluorophore or heterogeneous microenvironments are present, which is common in case of nucleic acid solutions. In order to mimic different chemical conditions present in nucleic acids, we used solvents of different polarity, solvent relaxation, and a collisional quencher to introduce heterogeneity into the 2AP microenvironment. To verify the effects of these chemical conditions in a biologically relevant system, we have also designed an RNA hairpin labeled with 2AP in the stem position. Finally, the effects of these different environmental conditions on the fluorescence of 2AP alone or in an RNA context are described by a lifetime distribution model and compared with classical exponential lifetime analysis.

2. MATERIALS AND METHODS

2AP was from Sigma and was used without further purification. Acrylamide (99.9% pure) was from BioRad. Dioxane and glycerol were from Fisher Biochemical and were of highest grade. The fluorescence background from the solvents used was less than 0.5% in all spectroscopic measurements. Percent mixtures of these solvents were prepared by weight. Neither the absorbance nor the intrinsic fluorescence of these solvents was altered during the experiments described. Titrations with acrylamide and dilutions were made directly in cuvettes and mixed either by stirring or inversion.

Synthetic RNA Oligonucleotides

RNA substrate (HP21) was synthesized, 2′-hydroxyl-deprotected, and purified by Dharmacon Research. The RNA oligonucleotide was resuspended in ultrapurified water and quantified by A260 in 10 mM potassium HEPES/acetic acid (pH 7.4) and 9 M urea, using extinction coefficient provided by Dharmacon. The extinction coefficient (ε_{260}) used was

232 200 L mol $^{-1}$ cm^{-1}. The RNA hairpin substrate (denoted HP21) was of the sequence 5 '-CAUACACGAAAGAAAUCGGU-2AP-UG-3'.

2.1 Steady-state fluorescence measurements

Absorption spectra were measured with a Varian Cary 50 spectrophotometer (Varian Inc.) in 1 cm × 1 cm quartz cuvettes over the range of 200–370 nm using an averaging time of 0.1 second. Fluorescence spectra were obtained using Varian Cary Eclipse spectrofluorometer (Varian Inc.) in 4 mm × 4 mm quartz cuvettes. Samples were excited at 303 nm and emission was measured over the range of 320–500 nm with 5 nm excitation and emission slits. At these wavelengths solvents and quencher used were found to have negligible fluorescence compared to 2AP.

2.2 Time-domain fluorescence measurements

Time-domain measurements were performed on a FluoTime 200 (Picoquant) equipped with a Hamamatsu microchannel plate (MCP) providing < 50 ps resolution. The emission monochromator was set to 370 nm, with the emission and excitation slits fully open, and polarizers set to magic angle conditions. The excitation source was a 295 nm LED driven at a 10 MHz repetition rate by a PDL800 driver (Picoquant) with a pulse width of ~500 ps. The excitation window was fitted with a 310 nm short pass filter; this prevented excitation wavelength leak to the detector since the LED produces a broad excitation spectrum. The emission side was equipped with a 350 nm long pass filter in front of the monochromator. Time-resolved fluorescence data were analyzed using the Fluofit software package v4.0 (Picoquant). Lifetime data were analyzed either by the exponential reconvolution procedure using nonlinear regression (multi-exponential model) or by lifetime distribution (Lorentzian model). In case of multi-exponential analysis, fluorescence decays were fitted to a sum of *n* exponentials,

$$I(t)=\sum_{i=1}^{n}\alpha_i e^{-(t/\tau_i)} \quad \text{(Eq. 1)}$$

where α_i is the fractional contribution of each component lifetime (τ_i). When more than one lifetime component is indicated, the amplitude-weighted average lifetime is reported as

$$\tau_{amp}=\sum_{i=1}^{n}\alpha_i\tau_i \quad \text{(Eq. 2)}$$

For lifetime distributions, fluorescence intensity total decays were sum of individual decays weighted by the amplitudes are fitted by

$$I(t)=\int_{\tau=0}^{\infty}\alpha(\tau)e^{-t/\tau}d\tau \quad \text{(Eq. 3)}$$

with distribution

$$\alpha(\tau)=\frac{A_i}{\pi}\frac{\Gamma_i/2}{(\tau-\overline{\tau}_i)^2+(\Gamma_i/2)^2} \quad \text{(Eq. 4)}$$

Here, A_i is the amplitude of the ith component, $\bar{\tau}_i$ is the central value of the ith, distribution and Γ_i is its full width at half maximum (FWHM). The use of the continuous distribution $\alpha(\tau)$ minimizes the number of floating parameters in the fitting algorithms.

3. RESULTS

3.1 Effect of microenvironment on 2AP lifetime distribution

Solvent polarity significantly influences the fluorescence spectra of polar dye molecules. Several theoretical models have been proposed to describe spectral shifts accompanying changes in solvent polarity [26–30]. These shifts are either due to general solvent effects like changes in dipole moment or refractive index, or to specific solvent effects like hydrogen bonding or formation of internal charge transfer (ICT)/twisted internal charge transfer (TICT) states [31,32]. Dipole moment and refractive index show opposite effects on spectral shift. For example, an increase in refractive index decreases energy loss and thus minimizes the spectral shift whereas an increase in dipole moment results in increased energy loss and spectral shift. Excitation forces charge separation in 2AP which causes an increase in dipole moment. Accordingly, dipole-dipole interactions between 2AP and polar solvents will divert energy from 2AP, resulting in red-shifted emission. Blue-shifted emission has also been reported for a 2AP-labeled DNA substrate upon addition of the DNA methyltransferase EcoKI [33].

Mixtures of polar and non-polar solvents are often used to characterize fluorophore spectral shifts. 2AP emission has been studied in mixtures of n-heptane:n-butanol, where the change in the dipole moment between ground and excited state was estimated as 2.5 Debye [34]. The shift of the emission maxima between non-polar and polar solvent was about 2000 cm^{-1}. Here, we have used dioxane and water as non-polar and polar contributors, respectively, to the local environment of 2AP. Dioxane:water mixtures induced both spectral shifts and changes in the fluorescence quantum yield of 2AP. Figure 1a shows normalized emission spectra of 2AP in dioxane, water and a mixture of 90% dioxane: 10% water. Only 10% of the polar solvent was required to induce 50% of the maximal spectral shift. Similarly, 10% water in the dioxane:water mixture resulted in an almost four-fold increase in emission intensity (Figure 1b). Specific solvent effects are mainly due to increases in hydrogen bonding which occur with very small (as low as 2%) increases in solvent polarity. In our experiments (not shown) we found that addition of such a low percentage of polar solvent does not cause significant spectral shift, which means that the effect is general rather than specific. This general effect may be due to the increase in solvent dipole moment which enhances energy loss from 2AP. By contrast, specific solvent effects would reflect the role of interactions like hydrogen bonding, experienced by all 2AP residues in double-stranded RNA or DNA environments, on 2AP photophysics. Here, the lack of specific dioxane effects on 2AP spectral shift suggests that hydrogen bonding does not significantly influence 2AP spectral shifts, consistent with findings reported elsewhere [8].

Next, we measured 2AP fluorescence intensity decays. Figure 2a shows the decays observed for 2AP in dioxane:water mixtures containing 0, 10 and 100% water. First, we fitted the intensity decay data to a multi-exponential model (Table 1). Whereas in neat solvents the decays can be well approximated with a single exponential model, in binary solvents two

components are required to fit the data. Heterogeneity in the 2AP intensity decay can be identified from the ratio of goodness-of-fit parameters (χ_R^2) for one- and two-exponent fits, with the greatest heterogeneity observed in mixtures containing 10% and 20% water. The heterogeneity of the intensity decay can be also visualized by the deviation of residuals from the single-exponential fit. Figure 2b shows minimal residual deviation from a single-exponential model for the intensity decay of 2AP in water (top), but significant deviation from a single-exponential fit when dissolved in a 90:10 mixture of dioxane:water (bottom) and a 80:20 mixture of dioxane:water (middle).

Though steady state spectral shifts and multi-exponential models of intensity decays are informative, the former has limited sensitivity while the latter is difficult to interpret. As such, these approaches are less useful for detecting minute alterations in the microenvironments surrounding 2AP, or just as importantly, changes in the range of microenvironments among a sampled population of 2AP molecules. As an alternative approach, we considered 2AP intensity decays using a Lorentzian lifetime distribution model (Eq. 3 and 4), which takes into consideration the average number of molecules emitting in different microenvironments, the range of mobility and polarity in each environment and the rate of change of environment around molecules [35–37]. Also, analysis of data by lifetime distribution model weights the data and thus is less sensitive to systematic errors [35–37]. Unlike the single-exponential decay model, a Lorentzian unimodal well approximates all intensity decays with goodness-of-fit parameters comparable to two-exponential model (comparing χ_R^2 in Tables 1 and 2). However, the FWHM values of the distribution strongly depend on the mixture (Figure 3 and Table 2), with the broadest distributions describing those 2AP samples most divergent from single-exponential intensity decay. Accordingly, the FWHM values of the lifetime distributions are clearly related to the microenvironmental heterogeneity of the 2AP sample.

3.2 Effect of fluorescence quenching on 2AP lifetime distribution

In many samples the intensity decays become non-exponential even when a single population of fluorophore is present; for example, in presence of quencher [38]. This effect where a single population of fluorophore shows non-exponential decay due to occasional quenching is known as the transient effect and it may be due to closely spaced fluorophore-quencher pairs. In the transient effect the lifetime decay is given by

$$I(t)=I_0\exp(-t/\tau - 2bt^{1/2}) \quad \text{(Eq. 5)}$$

In this expression *b* depends on quencher concentration and diffusion coefficient. Such decays can be resolved by multi-exponential models but that would be erroneous since the decays are non-exponential due to a distance-dependent occasional interaction with the quencher [39,40]. The best model to fit these non-exponential decays with a single exponent is a lifetime distribution model. We used acrylamide to quench 2AP fluorescence in a highly viscous solution (80:20 glycerol:water mixture) to detect the transient effect clearly [39,40]. One molar acrylamide quenches 2AP fluorescence by 50% with no detectable spectral shift (Figure 4). The fluorescence intensity decays of 2AP in the absence and presence of acrylamide are shown in Figure 5a and corresponding residual deviations are presented in

Figure 5b. The decay of 2AP fluorescence in presence of 1 M acrylamide shows a systematic deviation from the single-exponential model (Figure 5b, bottom panel) and clearly needs more than a single exponential fit. By contrast, these data were very well resolved using a single Lorentzian lifetime model, and show that the addition of acrylamide significantly broadens the lifetime distribution (Figure 6). Note that 80% glycerol broadened the FWHM from 0.7 ns in pure water (Table 2) to 2.6 ns (Figure 6), indicating the increase in heterogeneity upon addition of glycerol.

3.3 Effect of spectral relaxation on 2-AP lifetime distribution

Upon excitation a fluorophore either remains unrelaxed in a Frank-Condon state (F) or loses its energy and becomes relaxed (state R), the selection of which depends on its chemical structure and the nature of the local microenvironment. The two states F and R have their own characteristic lifetime decays; for example, a fluorophore in the F state exhibits a shorter lifetime than in the R state since the F state emits through both emission and relaxation. By contrast, an R state fluorophore emits only through emission, thus slowing the observed intensity decay [38,41,42]. Also, fluorophores in the F state emit at shorter wavelengths than in the R state where energy has been dissipated [41,42]. As such, a critical point to be considered in any measurement is whether the fluorophore is solvent relaxed or not. If so, emission should be measured at both shorter and longer wavelengths to avoid fluctuations in lifetimes due to interconversion between two states.

Here we have tried to see if 2AP undergoes solvent relaxation and after scanning over a range of wavelengths, we found that F state of 2AP emits at around 350 nm whereas R state emits at around 410 nm. Little heterogeneity was observed in 2AP fluorescence in the R state, since the intensity decay measured at 410 nm was well resolved by a single-exponential fit (Figure 7, top). However, similar to the heterogeneous intensity decays observed for 2AP in dioxane:water mixtures and in the presence of quencher (above), we observed that the intensity decay measured from the F state (350 nm) was very poorly approximated by the single-exponential function (Figure 7, bottom). By contrast, 2AP intensity decays from both the F and R states were well resolved by the unimodal Lorentzian distribution, with the most dramatic differences in emission properties reflected in the FWHM parameters. Furthermore, the large FWHM value for 2AP measured at the shorter wavelength (Figure 8) is consistent with increased heterogeneity of 2AP emission from the F state *versus* the R state. In previous studies, differences in fluorescence lifetime properties from F *versus* R states of the single tryptophan residue in staphylococcal nuclease revealed that local intramolecular dynamics create a polar environment around tryptophan rather than exposure to aqueous solvent [33]. Similarly, 2AP intensity decays from F and R states may help to predict the microenvironment around 2AP in different states. These data also provide a further example showing how the lifetime distribution approach can be used to describe heterogeneous 2AP intensity decays without the inclusion of additional exponential terms.

3.4 Effects of microenvironment, quenching and solvent relaxation on 2AP in RNA

In previous sections, we have evaluated the effects of microenvironment, quenching and solvent relaxation on 2AP in solvents. To study these effects in a biological sample, we utilized a synthetic 23 nucleotide RNA molecule capable of folding into a structurally

unambiguous hairpin [6] (Figure 9a). This RNA substrate is labeled with 2AP, which serves as a base analog of adenine and base pairs with T or U with a minimum perturbation in RNA structure [43,44].

To determine the effect of microenvironment on 2AP in RNA, we have compared the "HP21" RNA hairpin under native conditions (0 M Urea, 50 mM NaOAc and 5 mM $Mg(OAc)_2$) with its denatured form (7.5 M urea, 50 mM NaOAc and 0 mM $Mg(OAc)_2$). In the folded state, HP21 has a secondary structure where 2AP is able to base pair with uracil and can stack with base paired nearest neighbors (see Figure 9a). Collisions and stacking interactions between 2AP and adjacent bases, which are more pronounced within the native RNA state relative to the denatured state, generally tend to reduce the 2AP fluorescence lifetime [6,45]. As expected, 2AP in folded HP21 has a shorter average (amplitude-weighted, eq. 2) lifetime of 1.1 ns as compared to a 3.7 ns average lifetime of denatured RNA (Figure 9b, Table 3). Both native and denatured RNA have significantly shorter amplitude-weighted average lifetimes than free 2AP (τ_{amp} = 11.9 ns). In the samples tested here, 2AP is most strongly quenched in folded RNA, where the proximity of flanking and paired bases provides more opportunity for quenching interactions. Conversely, 2AP in a denatured RNA context experiences fewer quenching interactions, while free 2AP is least likely to be quenched. This change in lifetime supports our earlier results comparing free 2AP in water *versus* a water – dioxane mixture (Figure 2a) showing that the lifetime of 2AP is shorter in the heterogeneous microenvironment of a water – dioxane mixture. Similarly, Section 3.2 demonstrated that the presence of quencher shortens the 2AP lifetime and broadens the lifetime distribution.

While a single Lorentzian distribution described 2AP within denatured RNA, it did not adequately fit the data when the RNA was folded ($\chi_R^2 > 2.3$). Two distributions were required to describe the fluorescence decay, suggesting that heterogeneity is greatly enhanced relative to the denatured state. We found that an FWHM value in lifetime distribution analysis of denatured RNA (2.2 ns) is intermediate between the two distributions observed in native HP21 (0.10 ns and 5.5 ns). **A** broader FWHM for 2AP in the folded RNA indicates a more heterogeneous microenvironment around this fluorophore, possibly involving increased diversity of proximal stacking targets and RNA base-pair breathing dynamics. These two subpopulations for the native HP21 RNA may represent a fully stacked hybridized state of 2AP with a short lifetime and broad distribution in equilibrium with a partially open state where the terminal bases have a reduced likelihood of interactions with adjacent nucleotides, represented by a longer component lifetime and a narrower distribution. Evidence of this equilibrium was seen in our previous study [6]. The correlation of distribution breadth with environment complexity is consistent with our earlier finding that the lifetime distribution of 2AP in a homogeneous environment (water) is narrower than when in a heterogeneous environment (water – dioxane mixture) (Figure 3). Lorentzian analysis provides the distinct advantage of a more intuitive interpretation which describes the data with essentially equivalent χ_R^2 values, yet with a potentially significant decrease in model complexity: denatured HP21 requires 6 parameters with a 3-exponential fit as reported in Ballin *et al* [6], *versus* only 3 parameters for a Lorentzian distribution described here (Figure 9c).

4. DISCUSSION

Solvent polarity and local environment have profound effects on the emission spectral properties of 2AP. This local environment surrounding 2AP is basically composed of solvent components, for example bound proteins, salt and other buffer ingredients. These ingredients change the polarity around 2AP and thus cause alterations in its fluorescence properties. In nucleic acids, additional interactions are provided by adjacent bases [22]. These adjacent bases can cause both static and dynamic quenching similar to that caused by solvent interactions. In addition to quenching, solvent interaction can also cause spectral shift to longer or shorter wavelengths depending upon its polarity.

In this study, we mimicked several microenvironmental features that may be presented to 2AP in nucleic acid or nucleoprotein contexts and analyzed their effects on 2AP fluorescence lifetime properties using a lifetime distribution approach. Quenching interactions were modeled by addition of acrylamide, and 2AP spectral shifts which could result from protein interactions, etc. [22] were obtained by variation of solvent polarity. Measurement of 2AP intensity decays at multiple wavelengths further permitted the impact of spectral relaxation on lifetime properties to be assessed. To re-evaluate these effects on 2AP fluorescence properties in biological samples, the fluorescence decay of HP21 RNA hairpin was measured under native and denaturing conditions.

For all solvent interaction models tested in this study, significant heterogeneity was introduced into 2AP intensity decays either by mixing solvents of different polarities or by promoting folding of the RNA hairpin molecules. The conventional approach to interpret such data would be through multi-exponential regression solutions. However, resolution of measured 2AP intensity decays as a weighted sum of multiple discrete lifetimes is difficult to interpret. For example, some reports have indicated 4 or 5 discrete lifetimes for 2AP in a single sample, and the component lifetime values themselves can vary widely between data sets [19,46]. Furthermore, multi-exponential decays may hide sources of heterogeneity such as by superimposition of heterogeneous decays comprising individual lifetimes close to one another. Given the multitude of interactions possible in biological systems and the well documented sensitivities of 2AP and tryptophan to their microenvironment, there is little reason to believe that a sum of exponential terms truly represents the fluorescence decay of such fluorophores [36]. In fact, frequency domain time-resolved fluorescence studies revealed a more subtle danger of discrete multi-exponential lifetime analysis [37]. Prendergast and coworkers demonstrated that component lifetime parameters for multi-exponential decay fits exhibited extreme sensitivity to the number of data points collected and the frequencies over which the data was collected. By contrast, lifetime distribution analyses were found to be insensitive to the nature of data collection, and that the shape of asymmetric lifetime distributions were generally recoverable as the sum of symmetric distribution functions for the systems considered. In essence, lifetime distribution analysis is less sensitive to perturbing factors which serve to complicate multi-exponential analysis and the corresponding results are more likely to represent the underlying phenomena of interest in a way which is interpretable in terms of a structural model or mechanism.

A unimodal lifetime distribution model includes two floating parameters: the central (median) lifetime and the FWHM which defines the breadth of the distribution (Eqs. 3 and 4). The data presented in this study show that, for 2AP, both parameters can vary as a function of solution environment. For example, variations in solvent polarity altered both the central lifetime and FWHM parameters of 2AP lifetime distributions. Notably, these parameters were more sensitive to changes in solvent polarity than steady-state fluorescence measurements on comparable samples. The Lorentzian distributions describing 2AP lifetime properties in 50% dioxane: 50% water *versus* 100% water were clearly distinguishable (Figure 3), while the same samples exhibited virtually no difference in quantum yield (Figure 1b) or spectral position (*data not shown*).

Using the Lorentzian lifetime distribution model, heterogeneity in 2AP emission characteristics was directly reflected in resolved FWHM values. Increases in distribution breadth were observed in response to many different stimuli, indicating that this parameter may be a useful means of tracking changes in 2AP microenvironment. Application of Lorentzian distribution analysis to time-resolved fluorescence measurements detected evidence of conformational dynamics not readily apparent from either steady state fluorescence studies or *via* 3-component exponential analysis [6]. Extrapolating these findings to generalized studies of nucleic acids, we anticipate that lifetime distribution models will enhance the range and sensitivity of conformational events that may be visualized using 2AP-labeled nucleic acid substrates, including stimulus-dependent changes in DNA/RNA folding, conformational dynamics, or association with specific proteins.

ACKNOWLEDGEMENTS

This work was supported by Texas Emerging Technology Fund grant (to Z.G.), NIH/NCI grant CA102428 (to G.M.W.) and a competitive supplemental from the Division of Cancer Biology (NIH/NCI) under the Activities to Promote Research Collaborations initiative (to G.M.W). Additional support (for S. B.) was provided by Public Health Service Grant P20 MD001633.

REFERENCES

1. Doudna J. A molecular contortionist. Nature. 1997; 388:830–835. [PubMed: 9278040]
2. Hendrix DK, Brenner SE, Holbrook SR. RNA structural motifs: building blocks of a modular biomolecule. Q. Rev. Biophys. 2005; 38:221–243. [PubMed: 16817983]
3. Ward DC, Reich E, Stryer L. Fluorescence studies of nucleotides and polynucleotides. I. Formycin, 2-aminopurine riboside, 2,6-diaminopurine riboside, and their derivatives. J. Biol. Chem. 1969; 244:1228–1237. [PubMed: 5767305]
4. Smagowicz J, Wierzchowski KI. Lowest excited states of 2-aminopurine. J. Lumin. 1974; 8:210–232.
5. Sowers LC, Fazakerley GV, Eritja R, Kaplan BE, Goodman MF. Base pairing and mutagenesis: observation of a protonated base pair between 2-aminopurine and cytosine in an oligonucleotide by proton NMR. Proc. Natl. Acad. Sci. USA. 1986; 83:5434–5438. [PubMed: 3461441]
6. Ballin JD, Bharill S, Fialcowitz-White EJ, Gryczynski I, Gryczynski Z, Wilson GM. Site-specific variations in RNA folding thermodynamics visualized by 2-aminopurine fluorescence. Biochemistry. 2007; 46:13948–13960. [PubMed: 17997580]
7. Kawski A, Bartoszewicz B, Gryczynski I, Krarewski M. Dipole moment changes and composition of solvent shell of 2-Aminopurine derivatives. Bull. Pol. Acad. Sci. Ser. Sci. Math. Astr. et Phys. 1975; 23:367–372.

8. Rachofsky EL, Osman R, Ross JBA. Probing structure and dynamics of DNA with 2-aminopurine: effects of local environment on fluorescence. Biochemistry. 2001; 40:946–956. [PubMed: 11170416]
9. Bloom LB, Otto MR, Beecham JM, Goodman MF. Influence of 5'-nearest neighbors on the insertion kinetics of the fluorescent nucleotide analog 2-aminopurine by Klenow fragment. Biochemistry. 1993; 32:11247–11258. [PubMed: 8218190]
10. Hochstrasser RA, Carver TE, Sowers LC, Millar DP. Melting of a DNA helix terminus within the active site of a DNA polymerase. Biochemistry. 1994; 33:11971–11979. [PubMed: 7918416]
11. Sastry SS, Ross BM. A direct real-time spectroscopic investigation of the mechanism of open complex formation by T7 RNA polymerase. Biochemistry. 1996; 35:15715–15725. [PubMed: 8961934]
12. Zhong X, Patel SS, Werneberg BG, Tsai MD. DNA polymerase beta: multiple conformational changes in the mechanism of catalysis. Biochemistry. 1997; 36:11891–11900. [PubMed: 9305982]
13. Holz B, Klimasauskas S, Serva S, Wienhold E. 2-Aminopurine as a fluorescent probe for DNA base flipping by methyltransferases. Nucleic Acids Res. 1998; 26:1076–1083. [PubMed: 9461471]
14. Allan BW, Reich NO. Targeted base stacking disruption by the EcoRI DNA methyltransferase. Biochemistry. 1996; 35:14757–14762. [PubMed: 8942637]
15. Allan BW, Beecham JM, Lindstrom WL, Reich NO. Direct real time observation of base flipping by the EcoRI DNA methyltransferase. J. Biol. Chem. 1998; 273:2368–2373. [PubMed: 9442083]
16. Stivers JT, Pankiewicz KW, Watanbe KA. Kinetic mechanism of damage site recognition and uracil flipping by Escherichia coli uracil DNA glycosylase. Biochemistry. 1999; 38:952–963. [PubMed: 9893991]
17. Menger M, Tuschl T, Eckstein F, Porschke D. Mg(2+)-dependent conformational changes in the hammerhead ribozymes. Biochemistry. 1996; 35:14710–14716. [PubMed: 8942631]
18. Stivers JT. 2-Aminopurine fluorescence studies of base stacking interactions at abasic sites in DNA: metal-ion and base sequence effects. Nucleic Acids Res. 1998; 26:3837–3844. [PubMed: 9685503]
19. Guest CR, Hochstrasser RA, Sowers LC, Millar DP. Dynamics of mismatched base pairs in DNA. Biochemistry. 1991; 30:3271–3279. [PubMed: 2009265]
20. Holmén A, Nordén B, Albinsson B. Electronic Transition Moments of 2-Aminopurine. J. Am. Chem. Soc. 1997; 119:3114–3121.
21. Evans K, Xu D, Kim Y, Nordlund TM. 2-Aminopurine optical spectra: solvent, pentose ring, and DNA helix melting dependence. J. Fluoresc. 2:209–216. [PubMed: 24241715]
22. Rachofsky EL, Sowers L, Hawkins ML, Balis FM, Laws WR, Ross JBA. Emission kinetics of fluorescent nucleoside analogs. Proc. SPIE. 1998; 3256:68–75.
23. Kelley SO, Barton JK. Electron transfer between bases in double helical DNA. Science. 1999; 283:375–381. [PubMed: 9888851]
24. Hariharan C, Reha-Krantz LJ. Using 2-Aminopurine fluorescence to detect bacteriophage T4 DNA polymerase-DNA complexes that are important for primer extension and proofreading reactions. Biochemistry. 2005; 44:15674–15684. [PubMed: 16313170]
25. Tang GQ, Patel SS. Rapid Binding of T7 RNA Polymerase is followed by simultaneous bending and opening of the promoter DNA. Biochemistry. 2006; 45:4947–4956. [PubMed: 16605262]
26. Mataga N, KAifu Y, Kozumi M. Solvent effects upon fluorescence spectra and the dipole moments of excited molecules. Bull. Chem. Soc. Jpn. 1956; 29:465–470.
27. Mcrae EG. Theory of solvent effects on molecular electronic spectra, frequency shifts. J. Phys. Chem. 1957; 78:2934–2941.
28. Lippert E. Spectroskopische bestimmung des dipolomomentes aromatischer verbindugen im ersten angeregten singulettzustand. Z. Electrochem. 1957; 61:962–975.
29. Bakshiev NG. Universal molecular interactions and their effect on the position of the electronic spectra of the molecules in two component solutions. Theory (liquid solutions). Opt. Spectrosc. 1962; 10:379–385.
30. Bilot L, Kawasaki A. Zur theory des einflusses von loesungsmitteln auf die elektronenspektren der molekuele. Z. Naturforsch. A. 1962; 17:621–628.

31. Rotkiewicz K, Grellmann KH, Grabowski ZR. Reinterpretation of the anomalous fluorescense of p-n,n-dimethylamino-benzonitrile. Chem. Phys. Lett. 1973; 19:315–318.
32. Grabowski ZR, Rotkiewicz K, Siemiaczuk A. Dual fluorescence of donoracceptor molecules and the Twisted Intramolecular Charge Transfer (TICT) states. J Lumin. 1979; 18:420–424.
33. Su TJ, Connolly BA, Darlington C, Mallin R, Dryden DTF. Unusual 2-aminopurine fluorescence from a complex of DNA and the EcoKI methyltransferase. Nucleic Acids Res. 2004; 32:2223–2230. [PubMed: 15107490]
34. Gryczynski I, Kawski A. Investigations on dipole moments of some aminopurines and aminopyrimidines by solvatochromism. Bull. Acad. Polon. Sci. Ser. Sci. Math. Astr. Et Phys. 1974; 25:1189–1196.
35. Alcala JR, Gratton E, Prendergast FG. Resolvability of fluorescence lifetime distributions using phase fluorometry. Biophys. J. 1987; 51:587–596. [PubMed: 3580485]
36. Alcala JR, Gratton E, Prendergast FJ. Interpretation of fluorescence decay in proteins using continuous lifetime distributions. Biophys. J. 1987; 51:925–936. [PubMed: 3607213]
37. Alcala JR, Gratton E, Prendergast FG. Fluorescence lifetime distributions in proteins. Biophys. J. 1987; 51:597–604. [PubMed: 3580486]
38. Lackowicz, JR. Principles of fluorescence Spectroscopy. New York: Kluwer Academic/Plenum; 2006.
39. Lackowicz JR, Zelent B, Gryczynski I, Kusba J, Johnson ML. Distance dependent fluorescence quenching of tryptophan by acrylamide. Photochem and Photobiol. 1994; 60:205–214.
40. Lackowicz JR, Kusba J, Szmacinski H, Johnson ML, Gryczynski I. Distance dependent fluorescence quenching observed by frequency domain fluorometry. Chem. Phys. Lett. 1993; 206:455–463.
41. Demchenko A, Gryczynski I, Gryczynski Z, Wiczk W, Malak H, Fishman M. Intramolecular dynamics in the environment of the single tryptophan residue in staphylococcal nuclease. Biophys. Chem. 1993; 48:39–48. [PubMed: 8257766]
42. Demchenko, A. Ultraviolet spectroscopy of proteins. Berlin: Springer; 1986.
43. Law SM, Eritja R, Goodman MF, Breslauer KJ. Spectroscopic and calorimetric characterizations of DNA duplexes containing 2-Aminopurine. Biochemistry. 1996; 35:12329–12337. [PubMed: 8823167]
44. Nordlund TM, Andersson S, Nilsson L, Rigler R, Graeslund A, McLaughlin LW. Structure and dynamics of a fluorescent DNA oligomer containing the EcoRI recognition sequence: fluorescence, molecular dynamics, and NMR studies. Biochemistry. 1989; 28:9095–9103. [PubMed: 2605243]
45. Rist MJ, Marino JP. Fluorescent nucleotide base analogs as probes of nucleic acid structure, dynamics and interactions. Curr. Org. Chem. 2002; 6:775–793.
46. Gondert ME, Tinsley RA, Rueda D, Walter NG. Catalytic core structure of the trans-acting HDV ribozyme is subtly influenced by sequence variation outside the core. Biochemistry. 2006; 45:7563–7573. [PubMed: 16768452]

a

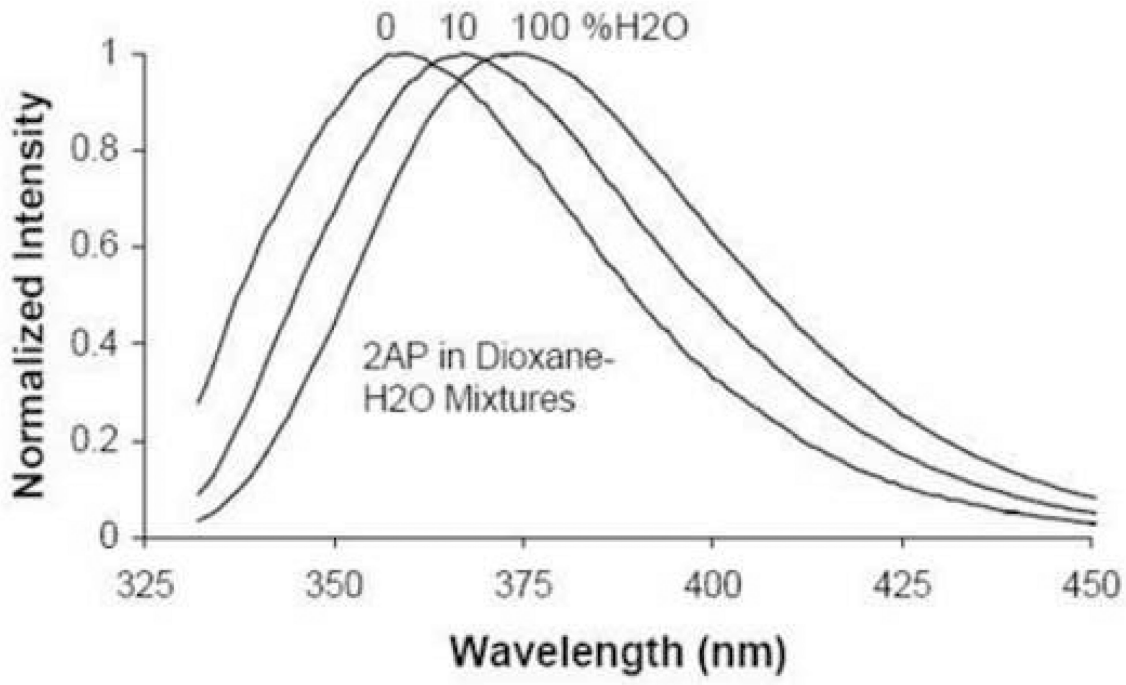

b

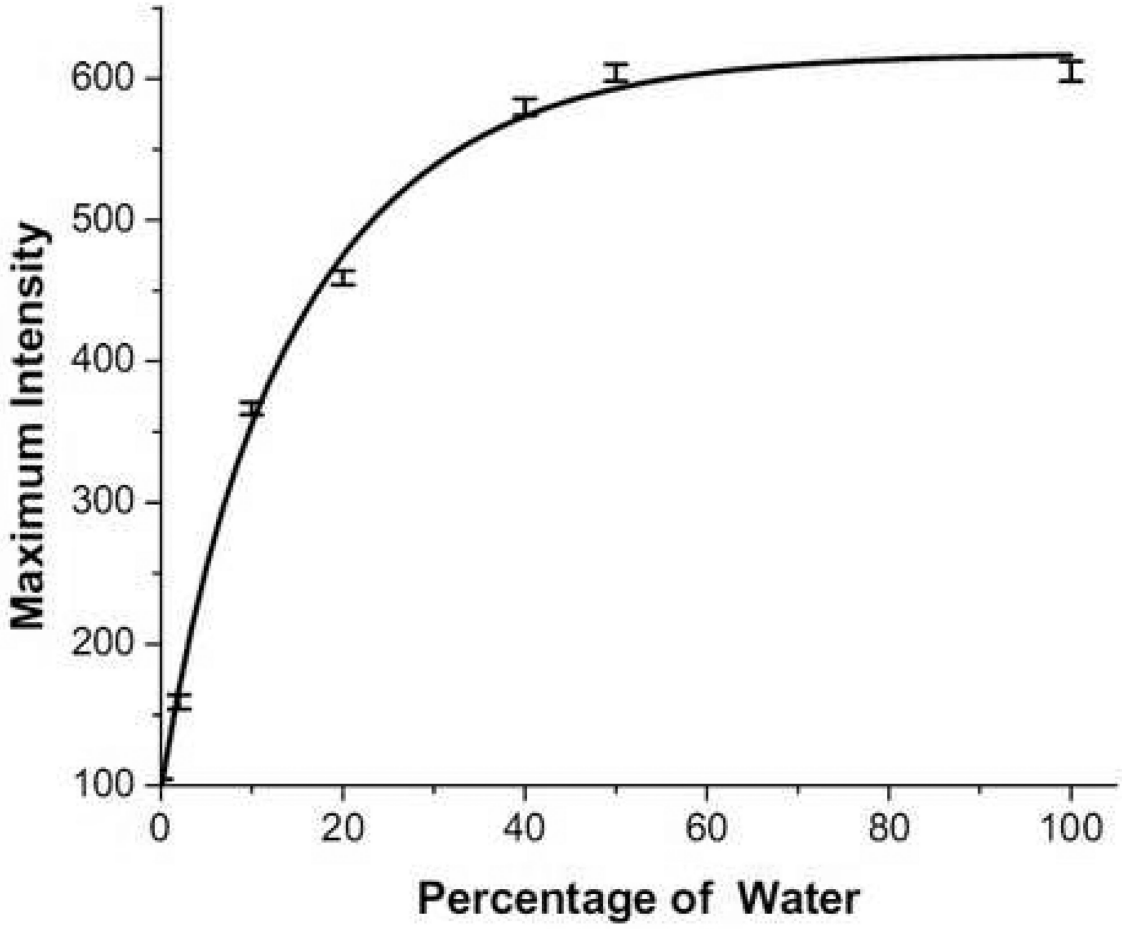

Figure 1.

1a. 2AP emission spectra in neat and binary solvents of dioxane and water. Left to right are spectra of 2AP solutions in dioxane, dioxane:water (90:10) and water alone. **1b**. Dependence of 2AP fluorescence intensity on the percentage of water in dioxane:water mixtures (n=3, Error = Mean ± SD). Fluorescence intensity increases with polarity resulting from addition of water in the mixture.

a

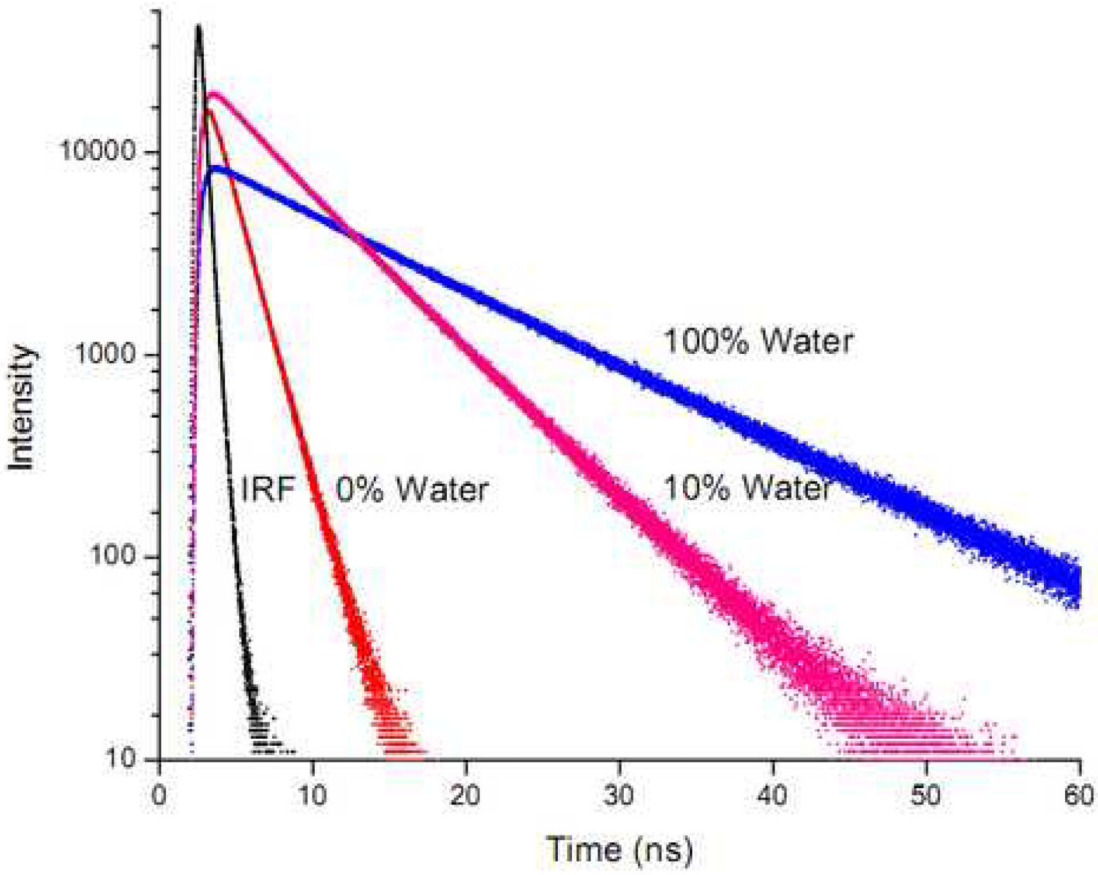

b

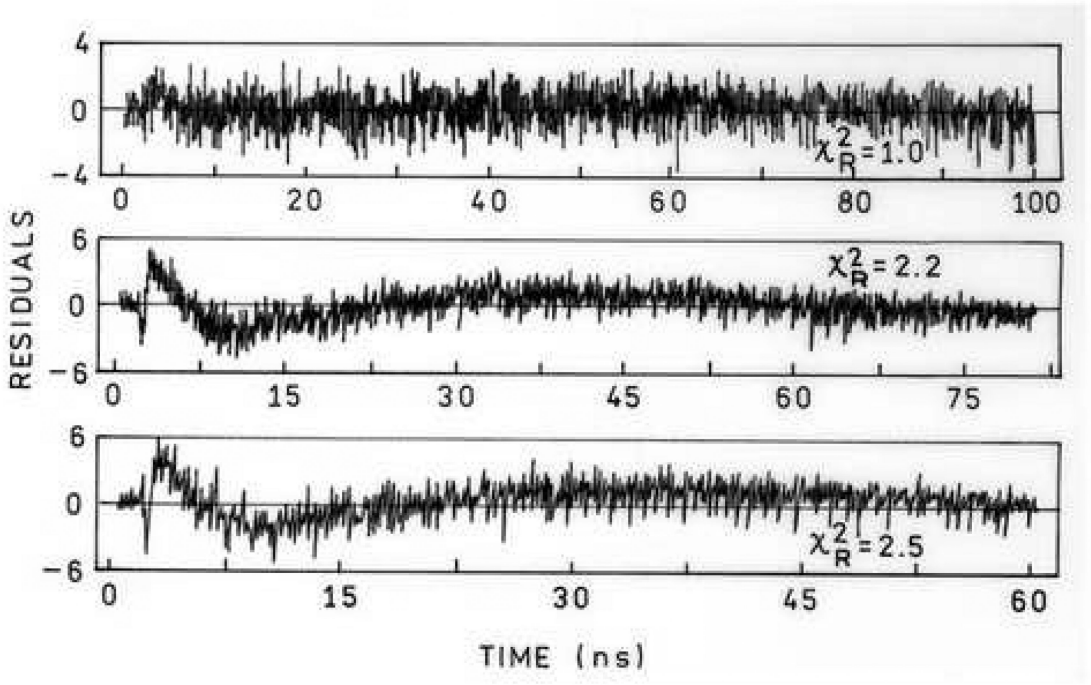

Figure 2.

2a. Fluorescence intensity decays of 2AP in neat and binary mixtures of dioxane and water. 2AP lifetime, as expected, is higher in water than in dioxane and dioxane:water mixtures.

2b. Deviations from the best-fits to the mono-exponential model of 2AP fluorescence intensity decays in water (top) and a dioxane:water mixture (90:10%; bottom and 80:20%; middle). Deviations are more pronounced in binary mixtures than in neat solvents because of higher heterogeneity in binary mixtures.

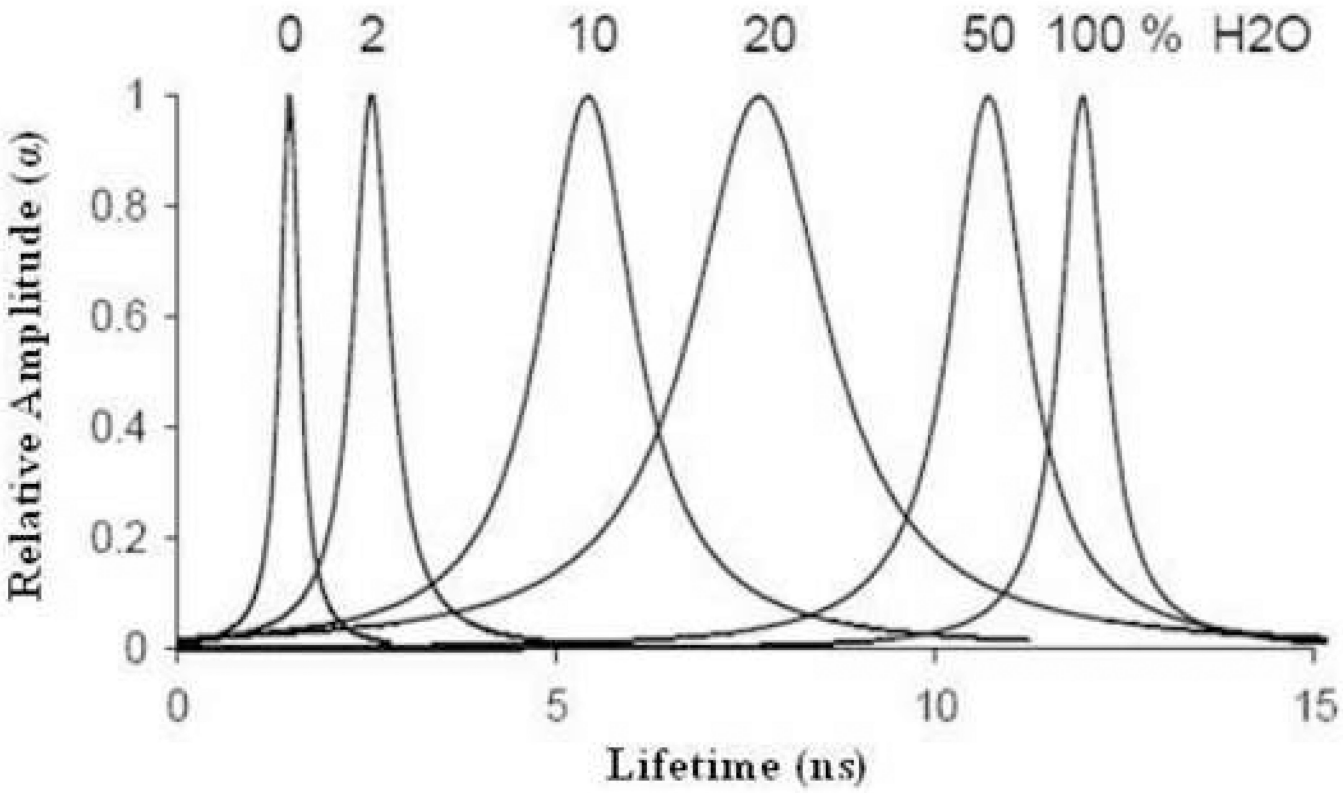

Figure 3.

Lifetime distributions (Lorentzian model) of 2AP fluorescence intensity decays in dioxane:water mixtures. Lifetime distributions are broader in highly heterogeneous mixtures (90:10% and 80:20% dioxane:water) than either in homogenous (100% and 0% water) or in less heterogeneous mixtures (98:2% dioxane:water).

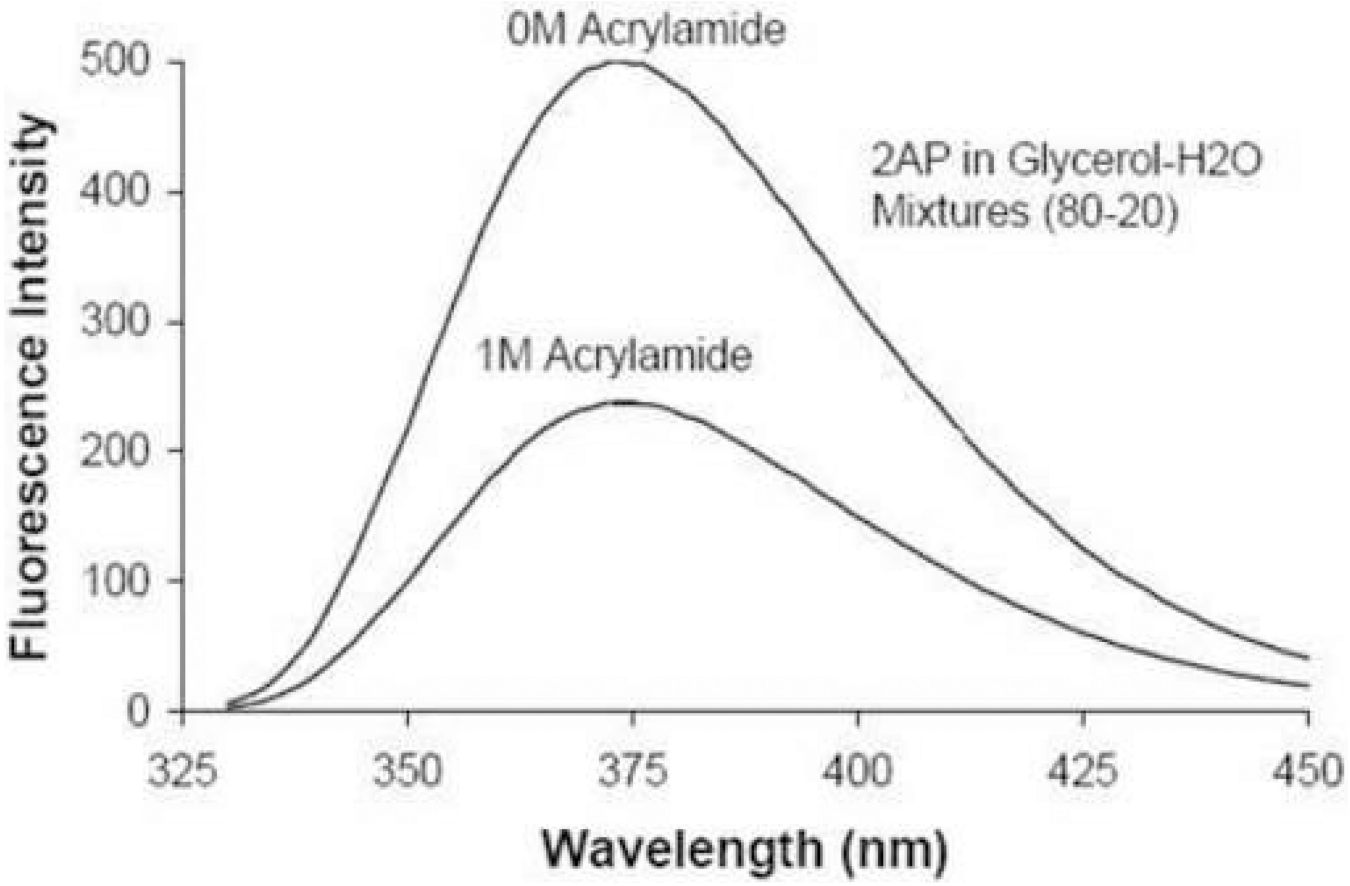

Figure 4.

Emission spectra of 2AP in absence and presence of 1 M acrylamide. Glycerol prevents the conformational changes in 2AP, if any, so that the effect of acrylamide can be exclusively detected.

a

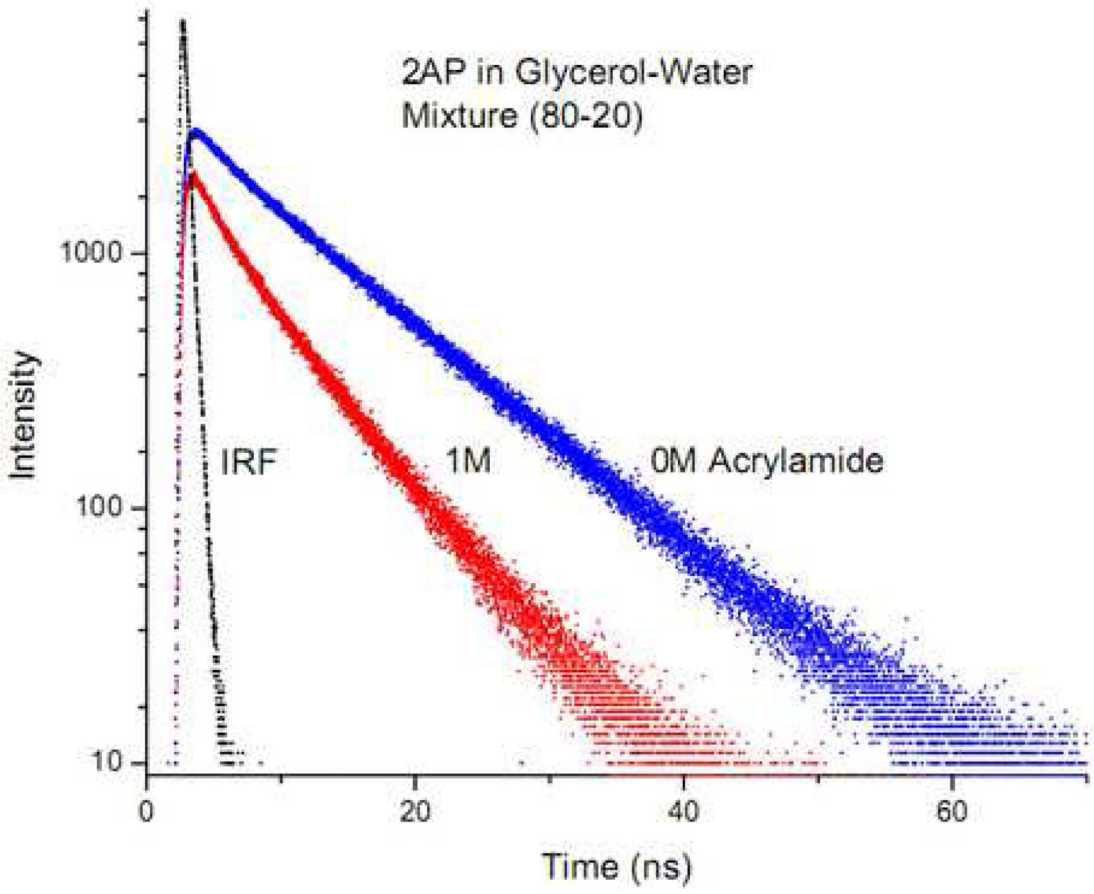

b

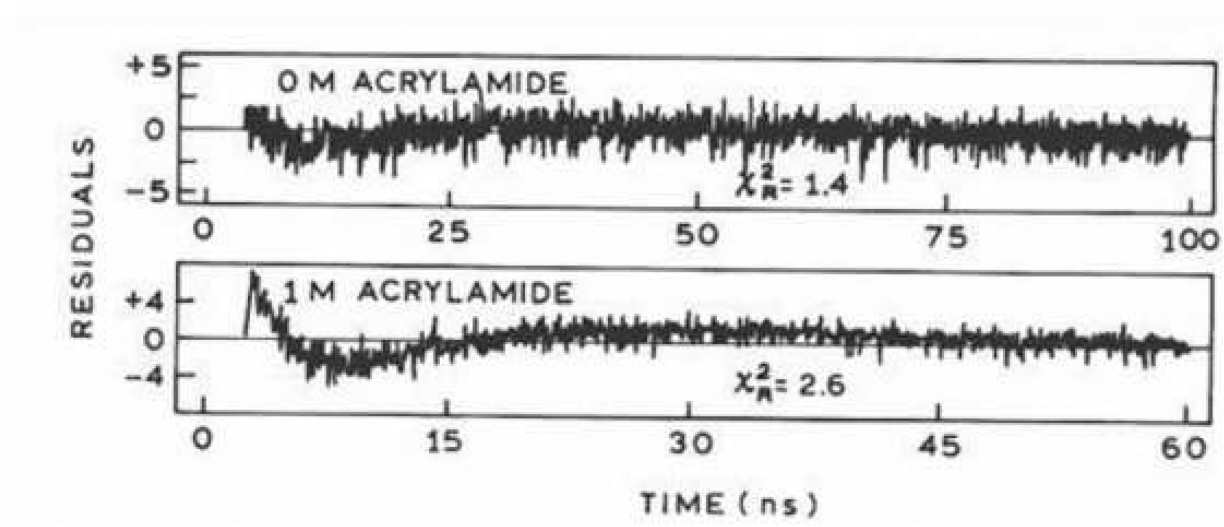

Figure 5.

5a. Fluorescence intensity decays of 2AP in presence and absence of 1 M acrylamide. Observation was made at 370 nm. **5b**. Deviations from the best fits to the mono-exponential model of 2AP fluorescence intensity decays in the absence and presence of 1 M acrylamide.

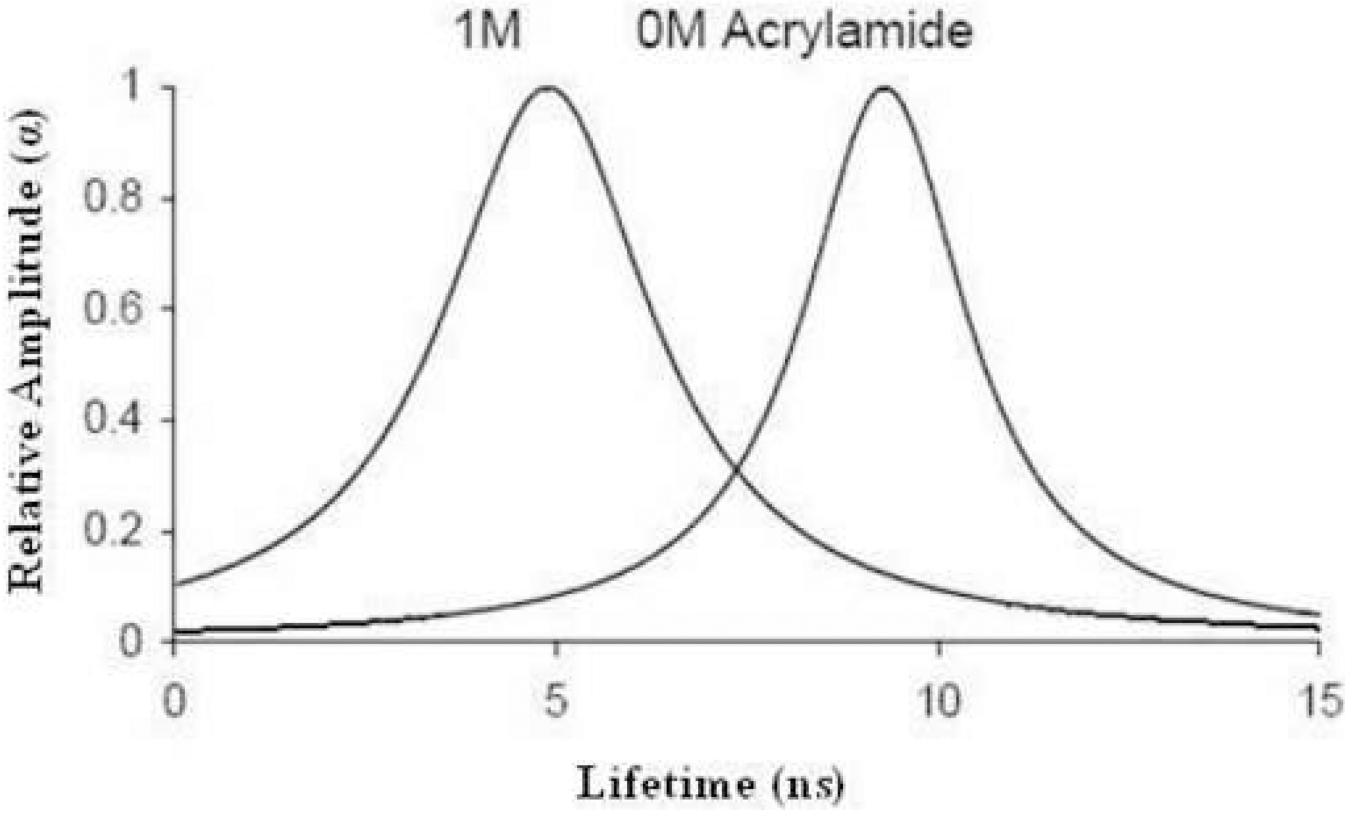

Figure 6.

Lifetime distributions (Lorentzian model) of 2AP intensity decays in presence and absence of 1M acrylamide. Addition of 1 M acrylamide broadens the lifetime distribution (FWHM) from 2.6 ns, χ_R^2=1.08 in 0 M acrylamide to 3.3 ns, χ_R^2=1.13 in 1 M acrylamide, owing to increased microenvironmental heterogeneity in 1 M acrylamide solution.

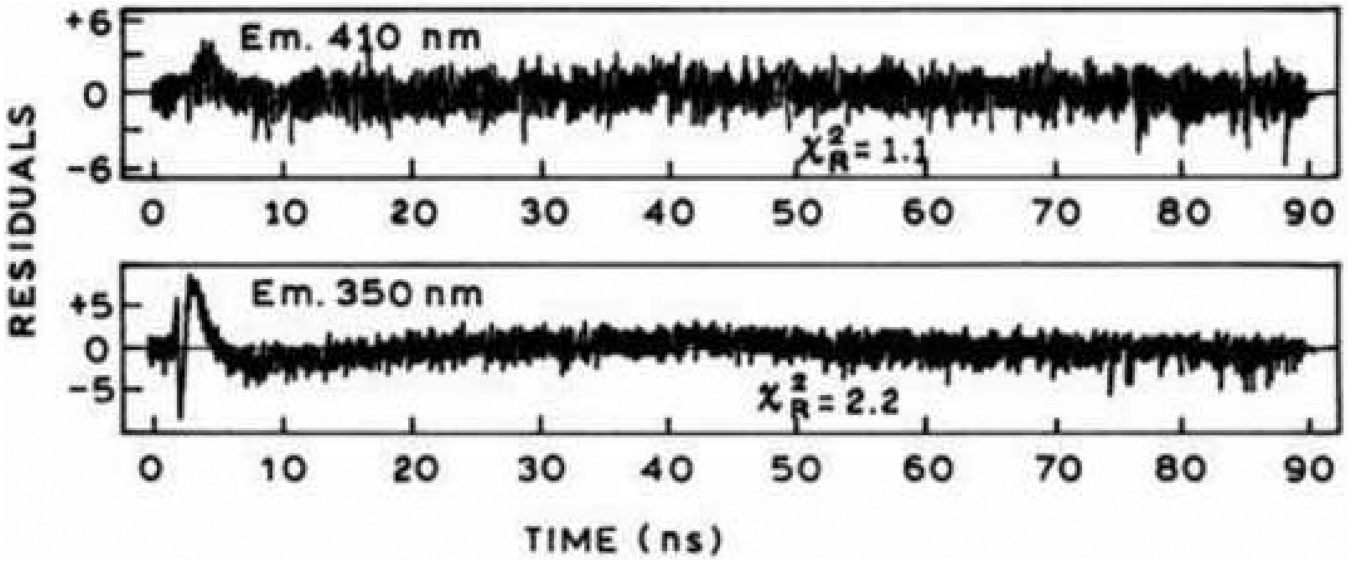

Figure 7.

Deviation from the best fits to the mono-exponential model of 2AP fluorescence intensity decays for various emission wavelengths. These measurements were done in glycerol at room temperature either at the long emission wavelength of 410 nm (top panel) or at short emission wavelength of 350 nm (bottom panel).

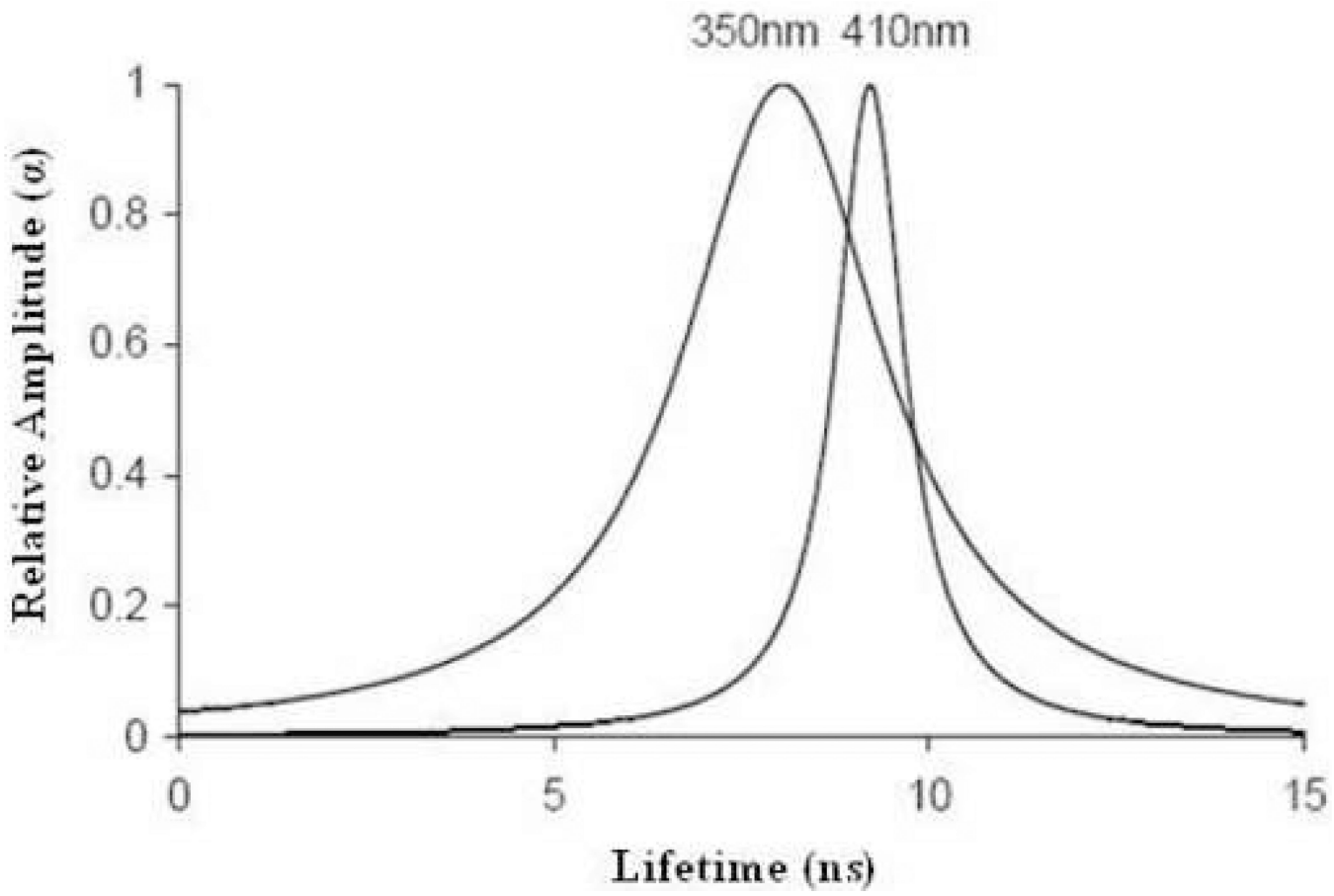

Figure 8.

Lifetime distribution (Lorentzian model) of 2AP fluorescence intensity decays for various emission wavelengths. These measurements were done in glycerol at room temperature either at the long emission wavelength of 410 nm (R state) or at short emission wavelength of 350 nm (F state). 2AP solution at 350 nm is more heterogeneous (FWHM = 3.2 ns, τ_0 = 7.89 ns, χ_R^2=1.53) than at 410 nm (FWHM = 1.1 ns, τ_0 = 9.14 ns, χ_R^2 =1.01).

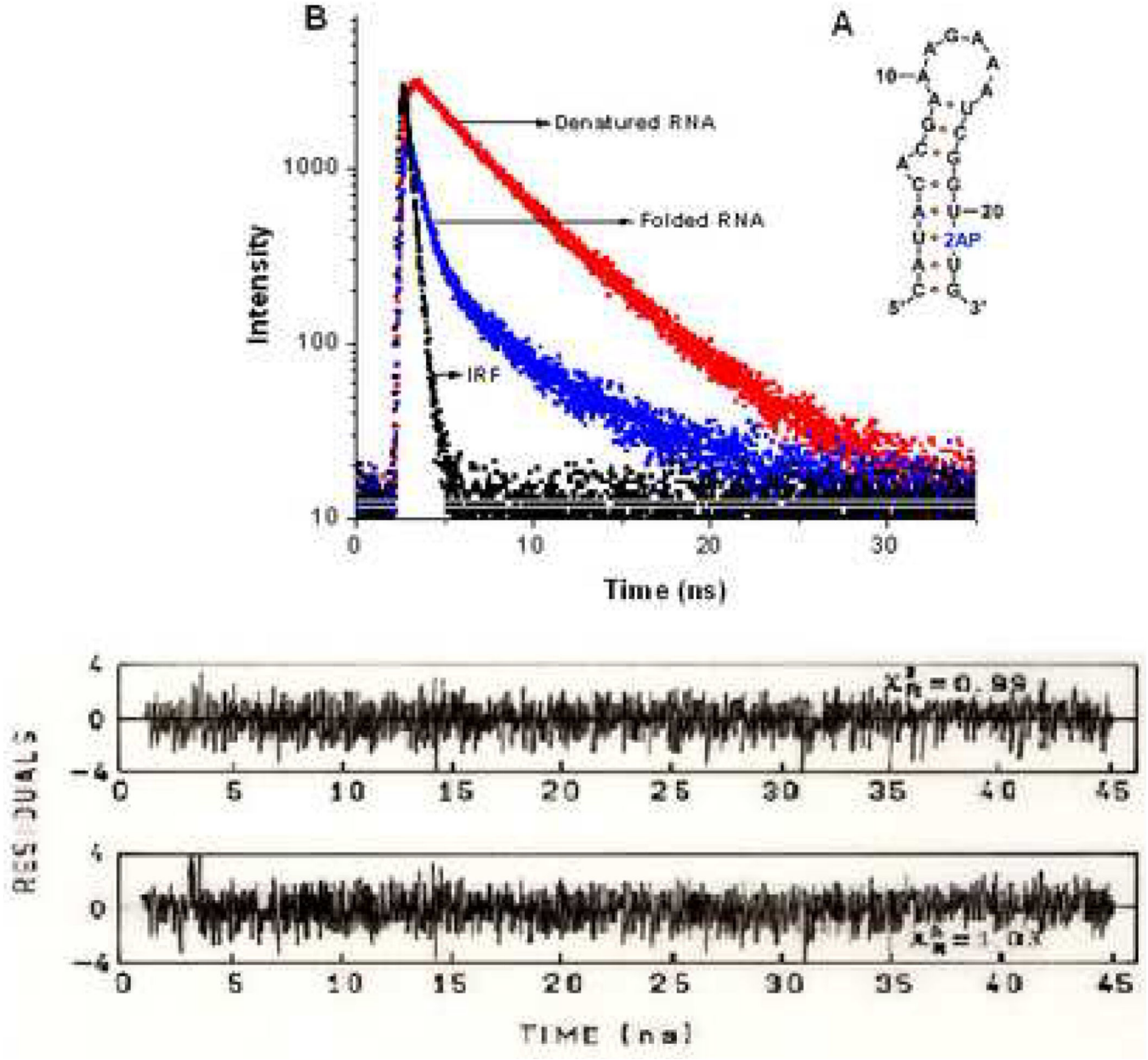

Figure 9.

9a. Synthetic RNA hairpin molecule "HP21" in folded state, labeled with 2AP at 21st position. **9b**. Fluorescence intensity decays of folded *versus* denatured RNA. **9c**. Top. Residuals from multi-exponential analysis (3 exponential fit, χ_R^2 = 0.99), Bottom. Residuals from Lorentzian lifetime distribution analysis (unimodal Lorentzian fit, χ_R^2= 1.03).

Table 1

Single *versus* multi-exponential analysis of 2AP fluorescence intensity decays in Dioxane:water mixtures

% of water	α_1	τ_1 (ns)	α_2	τ_2 (ns)	χ_R^2	χ_R^2 (exp1)/χ_R^2(exp2)
0	1.0	1.51±0.0046	-	-	1.21	1.44
	0.713	1.33±0.0064	0.287	1.80±0.0096	0.84	
2	1.0	2.62±0.0090	-	-	1.42	1.71
	0.353	1.90±0.0246	0.647	2.84±0.0089	0.83	
10	1.0	5.60±0.0218	-	-	2.52	2.52
	0.276	3.60±0.0621	0.724	6.06±0.0176	1.00	
20	1.0	6.81±0.0232	-	-	2.53	2.53
	0.275	4.36±0.0873	0.725	7.37±0.0180	1.00	
40	1.0	7.92±0.0305	-	-	2.41	2.36
	0.230	4.5±0.114	0.770	8.50±0.0238	1.02	
50	1.0	10.72±0.0462	-	-	1.16	1.25
	0.058	2.13±0.710	0.942	10.85±0.0459	0.93	
75	1.0	11.40±0.0249	-	-	0.98	1.05
	0.047	1.38±0.161	0.953	11.45±0.0573	1.03	
100	1.0	11.91±0.0505	-	-	1.03	1.01
	0.029	2.54±1.67	0.971	11.96±0.0477	1.01	

Table 2

Lifetime distribution analysis of 2AP fluorescence intensity decays in Dioxane: water mixtures using the Lorentzian model

% of Water	τ (ns)	FWHM* (ns)	χ_R^2
0	1.48±0.00383	0.30±0.0218	0.84
2	2.55±0.00628	0.59±0.0031	0.83
10	5.41±0.0137	1.50±0.0616	1.02
20	6.58±0.0174	1.79±0.0774	1.03
40	7.68±0.0207	2.16±0.0860	1.05
50	10.65±0.0452	1.21±0.0540	1.04
75	11.38±0.0345	0.83±0.0481	1.02
100	11.89±0.0548	0.70±0.0213	1.03

* full width at half maximum of Lorentzian distribution

Table 3

Lorentzian Lifetime distribution analysis of 2AP-Substituted RNA Substrates at 22°C in Folded *versus* Denatured Conformations[a]

	α_1[b] (%)	τ_1[b] (ns)	FWHM$_1$[b] (ns)	α_2[b] (%)	τ_2[b] (ns)	FWHM$_2$[b] (ns)	τ_{amp}[c] (ns)	χ_R^2[d]
Folded RNA	69 ± 3	0.17 ± 0.09	5.5 ± 0.1	31 ± 1	0.47 ± 0.02	0.1 ± 0.2	1.1	1.05
Denatured RNA	100	3.60 ± 0.06	2.2 ± 0.1	---	---	---	3.7	1.03

[a] Time-resolved fluorescence parameters were derived by resolution to a single or dual Lorentzian distribution (eq. 3–4). Native solution conditions were 50 mM NaOAc, 5 mM $Mg(OAc)_2$, 10 mM NaHEPES pH 7.4 whereas denaturing conditions were 50 mM NaOAc, 7.5 M urea, and 10 mM NaHEPES pH 7.4.

[b] Errors represent 67% confidence intervals based on support plane error analyses.

[c] Average amplitude-weighted lifetime, determined using eq. 2.

[d] Reduced χ^2 value for the nonlinear least squares analysis.